

Supporting Information

A novel iron complex for highly efficient catalytic hydrogen generation from the hydrolysis of organosilanes

Alan Kay Liang Teo and Wai Yip Fan*

Department of Chemistry, National University of Singapore,
3 Science Drive 3, Singapore 117543.

*Corresponding Author: Fax: (+65) 6779-1691. E-mail: chmfanwy@nus.edu.sg.

List of Figures and Tables

	Page
Fig. S1 IR Spectrum (in CH ₃ CN) of [Fe(C ₆ H ₅ N ₂ O)(CO)(MeCN) ₃][PF ₆].	S3
Table S1 Comparison of the catalytic performance of the hydrolytic oxidation of triethylsilane based on iron complex and other catalysts.	S5
Table S2 Sample and crystal data.	S7
Table S3 Data collection and structure refinement.	S8
Table S4 Atomic coordinates and equivalent isotropic atomic displacement parameters (Å ²).	S9
Table S5 Bond lengths (Å).	S10
Table S6 Bond angles (°).	S11
Table S7 Anisotropic atomic displacement parameters (Å ²).	S12
Table S8 Hydrogen atomic coordinates and isotropic atomic displacement parameters (Å ²).	S13
Table S9 Hydrogen bond distances (Å) and angles (°).	S13

Experimental

General

Syntheses were performed under nitrogen using standard Schlenk line techniques. Glassware was oven-dried for 3 hours at 150 °C prior to use. CD₃CN, CDCl₃, and D₂O were purchased from Cambridge Isotope Laboratory Inc. All other chemicals were obtained from Aldrich, Alfa Aesar, or Comac, and were used as received. NMR (¹H and ¹³C) spectra were recorded with a Bruker AC 300 Fourier transform spectrometer at room temperature. The chemical shifts (δ) were internally referenced to the residual solvent signals relative to tetramethylsilane. IR spectra were collected with liquid samples in a cell with CaF₂ windows and 0.1 mm path length, with a Shimadzu IR Prestige-21 spectrometer. Elemental analyses for carbon, hydrogen, and nitrogen were performed on an Elementar Vario Micro Cube elemental analyzer while iron concentration was determined by ICP analysis using a Perkin-Elmer Dualview Optima 5300 DV ICP-OES system at the Department of Chemistry, National University of Singapore. ESI mass spectra were measured using a Finnigan LCQ spectrometer. Hydrogen gas was detected using a Balzer Prisma QMS 200 residual mass analyzer and calibrated with known concentrations of pure hydrogen gas. The organic product yields were calculated from the ¹H NMR spectra using reagent grade toluene or *n*-hexane as internal standard.

Preparation of [Fe(C₆H₅N₂O)(CO)(MeCN)₃][PF₆]

To a completely frozen solution of triiron dodecacarbonyl (640 mg, 1.27 mmol) in dichloromethane (160 mL), iodine (968 mg, 7.62 mmol) in dichloromethane (320 mL) was added dropwise. The resulting solution was stirred for 15 minutes at room temperature. The color

of the solution turned from dark green to dark violet. 2-aminopyridine (359 mg, 3.81 mmol) was then added. Gas was evolved, and a dark green precipitate was formed over 45 minutes of stirring at room temperature. The solution was allowed to stir at room temperature for another 10 minutes until no bubbles were formed. Once the precipitation was completed, the solid was recovered with filtration and washed with hexane (80 mL). The resulting filtrate was dissolved in acetonitrile (60 mL) and left to stand for 45 minutes before silver hexafluorophosphate (964 mg, 3.81 mmol) was added and stirred for 5 minutes. Diethyl ether (100 mL) was then added to precipitate the product from the orange supernatant liquid. The product was recrystallized from slow cooling in diethyl ether to give $[\text{Fe}(\text{C}_6\text{H}_5\text{N}_2\text{O})(\text{CO})(\text{MeCN})_3][\text{PF}_6] \cdot \frac{1}{2}(\text{Et}_2\text{O})$ as orange crystals suitable for an X-ray diffraction study (933 mg, 1.82 mmol, 48%). IR (CH_3CN , cm^{-1}): 2077 (s). Anal. Calcd for $\text{C}_{13}\text{H}_{14}\text{N}_5\text{O}_2\text{FePF}_6$: C, 33.00; H, 2.98; N, 14.80; Fe, 11.80. Found: C, 32.65; H, 2.68; N, 14.55; Fe, 11.54. ESI-MS (CH_3OH , m/z): 320.7 $[\text{M} - \text{PF}_6 - \text{MeCN} + \text{MeOH}]^+$, 276.7 $[\text{M} - \text{PF}_6 - 2\text{MeCN} + \text{MeOH}]^+$.

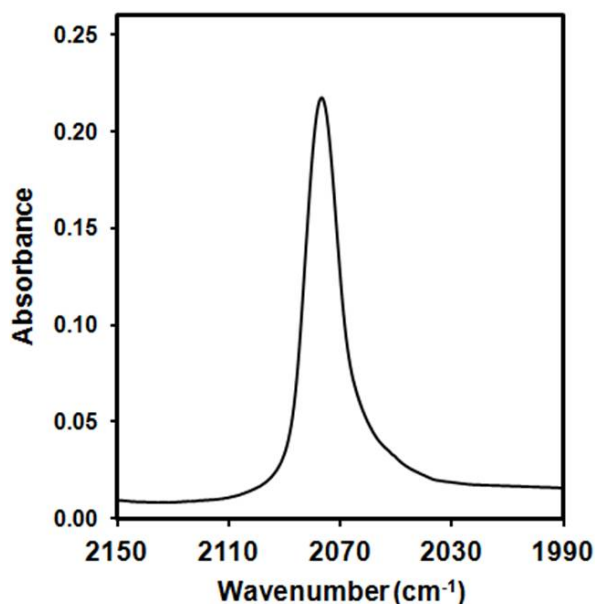


Fig. S1 IR Spectrum (in CH_3CN) of $[\text{Fe}(\text{C}_6\text{H}_5\text{N}_2\text{O})(\text{CO})(\text{MeCN})_3][\text{PF}_6]$.

Typical Procedure for Catalytic Reactions

Organosilane (2 mmol, 1 equiv) was added into a tetrahydrofuran (2 mL) solution containing the catalyst (0.2 μmol) and excess water (20 mmol). The reaction mixture was stirred under ambient conditions and evolution of gas was observed. Hydrogen gas was detected by sampling the headspace above the catalytic mixture throughout the reaction. A calibration curve using a known amount of pure hydrogen gas was used for the yield measurement. The yields of organosilanols were determined by ^1H NMR using reagent grade toluene or *n*-hexane as internal standard.

Product Identification

The generated gas in the oxidation reaction of organosilanes was identified to be dihydrogen gas by MS. The organosilanol products were identified by NMR through the comparison of their ^1H and ^{13}C NMR signals with the literature data: Et_3SiOH ,¹ *i*- Pr_3SiOH ,² PhMe_2SiOH ,³ Ph_2MeSiOH ,³ Ph_3SiOH .¹

Typical Procedure for Kinetic Studies

Triethylsilane was added into a tetrahydrofuran solution containing the catalyst and excess water. The reaction mixture was stirred under ambient conditions and the hydrogen released was measured volumetrically via the displacement of water from an inverted measuring cylinder. The reaction rate was determined by the initial rate of hydrogen evolution while the reaction orders were obtained by following the reaction rate at different concentration of reactants at 26.3 ± 0.3 °C. Kinetic isotope effect was determined by the ratio of the reaction rate of triethylsilane with H_2O and D_2O . Activation parameters were calculated from the rate

constants measured at different reaction temperature. The temperature was controlled by carefully adding ice into water. The effect of acetonitrile on the rate of hydrolysis was studied by comparing the reaction rate at different concentration of acetonitrile at 26.3 ± 0.3 °C.

Table S1. Comparison of the catalytic performance of the hydrolytic oxidation of triethylsilane based on iron complex and other catalysts..

Catalyst	Solvent	Time (min)	H ₂ (%)	Yield (%)	TON	TOF (hr ⁻¹)	Ref
[Fe(C ₆ H ₅ N ₂ O)(CO)(MeCN) ₃][PF ₆]	THF	15	99	> 99	10000	40000	This Work
[IrCl(C ₈ H ₁₂) ₂]	MeCN	60	-	80	80	80	(1)
[Re(O)(hoz) ₂][B(C ₆ F ₅) ₃]	MeCN	120	97	92	88	44	(4)
[RhCl(CO) ₂] ₂	THF	8	99	> 99	500	3750	(5)
[RuCl ₂ (<i>p</i> -cymene)] ₂	MeCN	10	-	95	48	288	(6)
Ru ₂ (CO) ₄ (PPh ₃) ₂ Br ₂	THF	60	71	60	1200	1200	(7)
Ru ₂ (CO) ₆ Br ₂	THF	5	83	75	1500	18000	(7)
Ru ₂ (CO) ₆ Cl ₄	THF	5	100	94	1880	22560	(7)
Carbon Nanotube–Gold Nanohybrids	THF	15	-	99	18000	72000	(8)
Nanoporous Gold	Acetone	120	-	94	94	47	(9)

X-ray Diffraction Studies

X-ray data for [Fe(C₆H₅N₂O)(CO)(MeCN)₃][PF₆] were collected with a Bruker D8 VENTURE PHOTON Diffractometer, using Mo K α radiation at 100(2) K with the SMART suite of programs.¹⁰ Data were processed and corrected for Lorentz and polarization effects with SAINT¹¹ and for absorption effects with SADABS.¹² Structural solution and refinement were carried out with the SHELXTL suite of programs.¹³ The structures were solved by direct methods to locate the heavy atoms, followed by difference maps for the light, non-hydrogen

atoms. All hydrogen atoms were placed in calculated positions. All non-hydrogen atoms were generally given anisotropic displacement parameters in the final model. The crystal structure report and a summary of the most important crystallographic data are provided in this Supporting Information.

Crystal Structure Report

A orange needle-like specimen of $C_{15}H_{19}F_6FeN_5O_{2.50}P$, approximate dimensions 0.048 mm \times 0.066 mm \times 0.178 mm, was used for the X-ray crystallographic analysis. The X-ray intensity data were measured.

The total exposure time was 6.46 hours. The frames were integrated with the Bruker SAINT software package using a narrow-frame algorithm. The integration of the data using a monoclinic unit cell yielded a total of 40849 reflections to a maximum θ angle of 27.50° (0.77 \AA resolution), of which 4849 were independent (average redundancy 8.424, completeness = 100.0%, $R_{\text{int}} = 17.01\%$, $R_{\text{sig}} = 10.76\%$) and 2923 (60.28%) were greater than $2\sigma(F^2)$. The final cell constants of $a = 14.3610(14) \text{ \AA}$, $b = 8.1428(7) \text{ \AA}$, $c = 18.0294(17) \text{ \AA}$, $\beta = 91.916(3)^\circ$, volume = $2107.2(3) \text{ \AA}^3$, are based upon the refinement of the XYZ-centroids of 294 reflections above $20 \sigma(I)$ with $5.235^\circ < 2\theta < 33.98^\circ$. Data were corrected for absorption effects using the multi-scan method (SADABS). The ratio of minimum to maximum apparent transmission was 0.872. The calculated minimum and maximum transmission coefficients (based on crystal size) are 0.8610 and 0.9600.

The structure was solved and refined using the Bruker SHELXTL Software Package, using the space group $P 1 2_1/c 1$, with $Z = 4$ for the formula unit, $C_{15}H_{19}F_6FeN_5O_{2.50}P$. The final anisotropic full-matrix least-squares refinement on F^2 with 293 variables converged at $R1$

= 7.30%, for the observed data and $wR2 = 16.32\%$ for all data. The goodness-of-fit was 1.060. The largest peak in the final difference electron density synthesis was $1.064 \text{ e}/\text{\AA}^3$ and the largest hole was $-1.497 \text{ e}/\text{\AA}^3$ with an RMS deviation of $0.121 \text{ e}/\text{\AA}^3$. On the basis of the final model, the calculated density was $1.608 \text{ g}/\text{cm}^3$ and $F(000)$, 1036 e^- .

Table S2. Sample and crystal data.

Chemical formula	$\text{C}_{15}\text{H}_{19}\text{F}_6\text{FeN}_5\text{O}_{2.50}\text{P}$	
Formula weight	510.17	
Temperature	100(2) K	
Wavelength	0.71073 \AA	
Crystal size	$0.048 \times 0.066 \times 0.178 \text{ mm}$	
Crystal habit	orange needle	
Crystal system	monoclinic	
Space group	P 1 21/c 1	
Unit cell dimensions	$a = 14.3610(14) \text{ \AA}$	$\alpha = 90^\circ$
	$b = 8.1428(7) \text{ \AA}$	$\beta = 91.916(3)^\circ$
	$c = 18.0294(17) \text{ \AA}$	$\gamma = 90^\circ$
Volume	$2107.2(3) \text{ \AA}^3$	
Z	4	
Density (calculated)	$1.608 \text{ g}/\text{cm}^3$	
Absorption coefficient	0.868 mm^{-1}	
$F(000)$	1036	

Table S3. Data collection and structure refinement.

Theta range for data collection	2.63 to 27.50°	
Index ranges	-18<=h<=18, -10<=k<=10, -23<=l<=23	
Reflections collected	40849	
Independent reflections	4849 [R(int) = 0.1701]	
Coverage of independent reflections	100.0%	
Absorption correction	multi-scan	
Max. and min. transmission	0.9600 and 0.8610	
Structure solution technique	direct methods	
Structure solution program	SHELXS-97 (Sheldrick 2008)	
Refinement method	Full-matrix least-squares on F ²	
Refinement program	SHELXL-2013 (Sheldrick, 2013)	
Function minimized	$\Sigma w(F_o^2 - F_c^2)^2$	
Data / restraints / parameters	4849 / 35 / 293	
Goodness-of-fit on F ²	1.060	
Δ/σ_{\max}	0.001	
Final R indices	2923 data; I>2 σ (I)	R1 = 0.0730, wR2 = 0.1435
	all data	R1 = 0.1450, wR2 = 0.1632
Weighting scheme	$w=1/[\sigma^2(F_o^2)+(0.0429P)^2+10.3187P]$ where $P=(F_o^2+2F_c^2)/3$	
Largest diff. peak and hole R.M.S. deviation from mean	1.064 and -1.497 eÅ ⁻³ 0.121 eÅ ⁻³	

Table S4. Atomic coordinates and equivalent isotropic atomic displacement parameters (\AA^2). $U(\text{eq})$ is defined as one third of the trace of the orthogonalized U_{ij} tensor.

	x/a	y/b	z/c	$U(\text{eq})$
Fe1	0.20225(5)	0.08252(9)	0.72481(4)	0.0163(2)
P1	0.40260(9)	0.74010(17)	0.92158(8)	0.0229(3)
F1	0.3539(3)	0.6206(4)	0.9778(2)	0.0514(11)
F2	0.4520(2)	0.8343(5)	0.9889(2)	0.0487(10)
F3	0.4508(2)	0.8613(5)	0.8654(2)	0.0504(10)
F4	0.3537(2)	0.6450(5)	0.8535(2)	0.0506(10)
F5	0.4900(2)	0.6189(4)	0.91775(19)	0.0401(9)
F6	0.3148(2)	0.8612(4)	0.92599(19)	0.0356(8)
O1	0.0172(2)	0.1506(4)	0.77385(19)	0.0219(8)
O2	0.1050(3)	0.9522(5)	0.5940(2)	0.0480(12)
N1	0.2344(3)	0.2880(5)	0.6745(2)	0.0154(9)
N2	0.0900(3)	0.3552(5)	0.7140(2)	0.0188(10)
N3	0.3262(3)	0.9734(5)	0.7070(2)	0.0230(10)
N4	0.2609(3)	0.1754(5)	0.8164(2)	0.0211(10)
N5	0.1668(3)	0.8971(6)	0.7844(2)	0.0243(10)
C1	0.3144(3)	0.3260(7)	0.6404(3)	0.0215(12)
C2	0.3284(4)	0.4750(6)	0.6089(3)	0.0221(12)
C3	0.2590(4)	0.5929(7)	0.6108(3)	0.0250(12)
C4	0.1775(4)	0.5581(6)	0.6461(3)	0.0221(12)
C5	0.1678(3)	0.4027(6)	0.6773(3)	0.0163(10)
C6	0.0874(3)	0.1964(6)	0.7430(3)	0.0158(10)
C7	0.1456(4)	0.0021(7)	0.6446(3)	0.0261(13)
C8	0.3933(4)	0.9021(7)	0.7016(3)	0.0261(12)
C9	0.4786(4)	0.8071(9)	0.6931(4)	0.0508(11)
C10	0.2989(4)	0.2082(7)	0.8705(3)	0.0230(12)
C11	0.3475(5)	0.2417(9)	0.9411(4)	0.0508(11)
C12	0.1494(4)	0.7941(8)	0.8224(3)	0.0320(15)
C13	0.1299(5)	0.6588(9)	0.8736(4)	0.0508(11)
O1S	0.9898(7)	0.9629(8)	0.9941(6)	0.032(2)
C1S	0.8954(10)	0.7333(15)	0.0235(8)	0.042(4)
C2S	0.9163(8)	0.9116(15)	0.0424(6)	0.032(3)
C3S	0.0106(9)	0.1357(10)	0.0082(7)	0.037(3)
C4S	0.0938(9)	0.178(2)	0.9630(8)	0.041(4)

Table S5. Bond lengths (Å).

Fe1-C7	1.761(6)	Fe1-C6	1.930(5)
Fe1-N5	1.931(5)	Fe1-N1	1.966(4)
Fe1-N4	1.979(5)	Fe1-N3	2.025(4)
P1-F2	1.583(3)	P1-F1	1.585(4)
P1-F3	1.590(4)	P1-F4	1.594(4)
P1-F5	1.600(3)	P1-F6	1.604(3)
O1-C6	1.225(6)	O2-C7	1.141(6)
N1-C5	1.339(6)	N1-C1	1.358(6)
N2-C5	1.373(6)	N2-C6	1.396(6)
N3-C8	1.131(6)	N4-C10	1.133(6)
N5-C12	1.117(7)	C1-C2	1.357(7)
C2-C3	1.384(7)	C3-C4	1.380(7)
C4-C5	1.394(7)	C8-C9	1.461(8)
C10-C11	1.457(8)	C12-C13	1.471(8)
O1S-C2S	1.453(8)	O1S-C3S	1.458(9)
C1S-C2S	1.519(9)	C3S-C4S	1.507(9)

Table S6. Bond angles (°).

C7-Fe1-C6	86.8(2)	C7-Fe1-N5	92.4(2)
C6-Fe1-N5	92.21(19)	C7-Fe1-N1	92.7(2)
C6-Fe1-N1	83.37(18)	N5-Fe1-N1	173.05(18)
C7-Fe1-N4	177.6(2)	C6-Fe1-N4	90.98(19)
N5-Fe1-N4	87.00(18)	N1-Fe1-N4	87.71(17)
C7-Fe1-N3	95.2(2)	C6-Fe1-N3	177.18(19)
N5-Fe1-N3	89.70(17)	N1-Fe1-N3	94.53(17)
N4-Fe1-N3	87.05(17)	F2-P1-F1	90.2(2)
F2-P1-F3	89.7(2)	F1-P1-F3	179.4(2)
F2-P1-F4	179.5(2)	F1-P1-F4	90.1(2)
F3-P1-F4	90.0(2)	F2-P1-F5	90.01(18)
F1-P1-F5	90.7(2)	F3-P1-F5	89.8(2)
F4-P1-F5	89.6(2)	F2-P1-F6	89.81(18)
F1-P1-F6	88.91(19)	F3-P1-F6	90.6(2)
F4-P1-F6	90.58(19)	F5-P1-F6	179.6(2)
C5-N1-C1	118.4(4)	C5-N1-Fe1	113.4(3)
C1-N1-Fe1	128.2(3)	C5-N2-C6	118.3(4)
C8-N3-Fe1	173.8(5)	C10-N4-Fe1	170.9(4)
C12-N5-Fe1	175.7(5)	C2-C1-N1	122.1(5)
C1-C2-C3	119.6(5)	C4-C3-C2	119.4(5)
C3-C4-C5	118.1(5)	N1-C5-N2	114.6(4)
N1-C5-C4	122.5(4)	N2-C5-C4	123.0(5)
O1-C6-N2	119.0(4)	O1-C6-Fe1	130.7(4)
N2-C6-Fe1	110.4(3)	O2-C7-Fe1	176.9(5)
N3-C8-C9	178.4(6)	N4-C10-C11	177.1(6)
N5-C12-C13	177.9(6)	C2S-O1S-C3S	108.8(8)
O1S-C2S-C1S	106.4(8)	O1S-C3S-C4S	106.7(9)

Table S7. Anisotropic atomic displacement parameters (\AA^2).

The anisotropic atomic displacement factor exponent takes the form:

$$-2\pi^2[h^2 a^{*2} U_{11} + \dots + 2 h k a^* b^* U_{12}]$$

	U_{11}	U_{22}	U_{33}	U_{23}	U_{13}	U_{12}
Fe1	0.0137(3)	0.0134(4)	0.0216(4)	0.0017(3)	-0.0024(3)	-0.0002(3)
P1	0.0183(7)	0.0188(7)	0.0316(8)	-0.0022(6)	-0.0012(6)	0.0007(6)
F1	0.054(2)	0.033(2)	0.070(3)	0.0161(19)	0.030(2)	0.0107(18)
F2	0.0317(19)	0.056(2)	0.057(2)	-0.032(2)	-0.0185(17)	0.0154(18)
F3	0.038(2)	0.051(2)	0.063(3)	0.019(2)	0.0094(18)	-0.0075(18)
F4	0.040(2)	0.057(2)	0.055(2)	-0.027(2)	-0.0117(18)	-0.0052(19)
F5	0.0300(18)	0.039(2)	0.051(2)	-0.0099(18)	0.0058(16)	0.0141(16)
F6	0.0204(16)	0.0245(17)	0.061(2)	-0.0009(17)	-0.0052(16)	0.0056(14)
O1	0.0140(18)	0.0217(19)	0.030(2)	0.0059(17)	0.0034(16)	-0.0016(15)
O2	0.054(3)	0.038(3)	0.050(3)	-0.013(2)	-0.026(2)	0.004(2)
N1	0.015(2)	0.014(2)	0.017(2)	-0.0024(18)	-0.0004(17)	-0.0018(17)
N2	0.015(2)	0.014(2)	0.027(2)	0.0031(19)	0.0023(19)	0.0003(18)
N3	0.021(2)	0.018(2)	0.030(3)	0.004(2)	-0.001(2)	0.000(2)
N4	0.014(2)	0.021(2)	0.029(3)	0.004(2)	0.0021(19)	0.0009(18)
N5	0.013(2)	0.027(3)	0.032(3)	0.004(2)	-0.0071(19)	0.001(2)
C1	0.016(3)	0.025(3)	0.024(3)	-0.002(2)	0.008(2)	0.000(2)
C2	0.020(3)	0.023(3)	0.024(3)	-0.005(2)	0.011(2)	-0.002(2)
C3	0.030(3)	0.017(3)	0.029(3)	0.000(2)	0.006(2)	-0.006(2)
C4	0.021(3)	0.014(3)	0.031(3)	-0.003(2)	0.005(2)	-0.002(2)
C5	0.016(2)	0.015(3)	0.018(2)	-0.002(2)	-0.0013(19)	-0.003(2)
C6	0.015(2)	0.011(2)	0.021(3)	0.001(2)	-0.005(2)	-0.003(2)
C7	0.026(3)	0.017(3)	0.035(3)	0.001(3)	-0.004(3)	0.004(2)
C8	0.020(3)	0.021(3)	0.037(3)	0.002(3)	0.003(2)	0.002(2)
C9	0.037(2)	0.051(3)	0.063(3)	0.021(2)	-0.012(2)	-0.010(2)
C10	0.017(3)	0.029(3)	0.023(3)	0.006(2)	0.001(2)	-0.005(2)
C11	0.037(2)	0.051(3)	0.063(3)	0.021(2)	-0.012(2)	-0.010(2)
C12	0.017(3)	0.037(4)	0.041(3)	0.024(3)	-0.012(3)	-0.013(3)
C13	0.037(2)	0.051(3)	0.063(3)	0.021(2)	-0.012(2)	-0.010(2)
O1S	0.031(4)	0.032(5)	0.034(4)	-0.008(4)	0.004(3)	0.003(4)
C1S	0.040(6)	0.041(6)	0.045(6)	-0.005(5)	0.013(5)	0.003(5)
C2S	0.031(5)	0.037(5)	0.029(4)	0.004(4)	0.003(4)	0.004(4)
C3S	0.040(5)	0.036(5)	0.035(5)	0.001(4)	-0.002(4)	0.003(4)
C4S	0.038(6)	0.038(7)	0.047(6)	-0.008(6)	0.005(5)	-0.007(6)

Table S8. Hydrogen atomic coordinates and isotropic atomic displacement parameters (Å²).

	x/a	y/b	z/c	U(eq)
H2N	0.041(4)	0.416(8)	0.712(3)	0.040(18)
H1	0.3623	0.2457	0.6385	0.026
H2	0.3853	0.4983	0.5858	0.027
H3	0.2675	0.6968	0.5880	0.03
H4	0.1294	0.6377	0.6490	0.026
H9A	0.4793	-0.2386	0.6429	0.076
H9B	0.4808	-0.2825	0.7294	0.076
H9C	0.5328	-0.1212	0.7014	0.076
H11A	0.3031	0.2369	0.9812	0.076
H11B	0.3756	0.3512	0.9397	0.076
H11C	0.3964	0.1593	0.9499	0.076
H13A	0.1468	-0.4458	0.8509	0.076
H13B	0.0635	-0.3419	0.8842	0.076
H13C	0.1666	-0.3260	0.9200	0.076
H1SA	0.8454	0.6932	0.0545	0.063
H1SB	0.9515	0.6670	0.0327	0.063
H1SC	0.8758	0.7248	-0.0289	0.063
H2SA	0.8601	0.9802	0.0338	0.039
H2SB	0.9370	0.9221	0.0952	0.039
H3SA	1.0251	1.1539	0.0616	0.045
H3SB	0.9567	1.2050	-0.0069	0.045
H4SA	1.1103	1.2935	-0.0292	0.062
H4SB	1.0785	1.1593	-0.0897	0.062
H4SC	1.1466	1.1083	-0.0215	0.062

Table S9. Hydrogen bond distances (Å) and angles (°).

	Donor-H	Acceptor-H	Donor-Acceptor	Angle
N2-H2N...O1	0.86(6)	2.10(6)	2.868(6)	148.0

References:

- 1 Y. Lee, D. Seomoon, S. Kim, H. Han, S. Chang, P. H. Lee, *J. Org. Chem.*, 2004, **69**, 1741-1743.
- 2 W. Adam, C. M. Mitchell, C. R. Saha-Mo1ller, O. Weichold, *J. Am. Chem. Soc.*, 1999, **121**, 2097-2103.
- 3 J. John, E. Gravel, A. Hagege, H. Li, T. Gacoin, E. Doris, *Angew. Chem. Int. Ed.*, 2011, **50**, 7533-7536.

- 4 R. A. Corbin, E. A. Ison, M. M. Abu-Omar, *Dalton Trans.*, 2009, **15**, 2850-2855.
- 5 M. Yu, H. Jing, X. Fu, *Inorg. Chem.*, 2013, **52**, 10741-10743.
- 6 M. Lee, S. Ko, S. Chang, *J. Am. Chem. Soc.*, 2000, **122**, 12011-12012
- 7 S. T. Tan, J. W. Kee, W. Y. Fan, *Organometallics*, 2011, **30**, 4008-4013
- 8 J. John, E. Gravel, A. Hagege, H. Li, T. Gacoin, E. Doris, *Angew. Chem. Int. Ed.*, 2011, **50**, 7533-7536.
- 9 N. Asao, Y. Ishikawa, N. Hatakeyama, Menggenbateer, Y. Yamamoto, M. Chen, W. Zhang, A. Inoue, *Angew. Chem. Int. Ed.*, 2010, **49**, 10093-10095.
- 10 SMART version 5.628; Bruker AXS Inc., Madison, WI, 2001.
- 11 SAINT+ version 6.22a; Bruker AXS Inc., Madison, WI, 2001.
- 12 Sheldrick, G. W. SADABS version 2.10; University of Göttingen, Göttingen, Germany, 2001.
- 13 SHELXTL version 6.14; Bruker AXS Inc., Madison, WI, 2000.